Supplementary Information for Dimensional crossover of class D real-space topological invariants

Martin Rodriguez-Vega,[1,*] Terry A. Loring,[2,†] and Alexander Cerjan[3,‡]

[1] *American Physical Society, 1 Physics Ellipse Dr, College Park, MD, USA*

[2] *Department of Mathematics and Statistics, University of New Mexico, Albuquerque, NM, USA*

[3] *Center for Integrated Nanotechnologies, Sandia National Laboratories, Albuquerque, NM, USA*

[*] rodriguezvega.physics@gmail.com

[†] tloring@unm.edu

[‡] awcerja@sandia.gov

SUPPLEMENTARY NOTE 1. DIMENSIONAL CROSSOVER OF CLASS BDI REAL-SPACE TOPOLOGICAL INVARIANTS

In this section, we consider the one-to-zero dimensional crossover of class BDI real-space topological invariants. Systems in this class possess particle-hole, time-reversal, and chiral symmetries. In 1D, the topological invariant corresponds to $\mathbb{Z}$, while in 0D corresponds to $\mathbb{Z}_2$. Zero-dimensional class BDI quantum dots and mechanical systems have been studied theoretically in Ref. [1]. As an example, we consider the Su–Schrieffer–Heeger (SSH) with a tight-binding Hamiltonian [2]

$$H = \sum_{i=1}^{N} v(c_{i,A}^{\dagger} c_{i,B} + h.c.) + \sum_{i=1}^{N-1} w(c_{i,B}^{\dagger} c_{i+1,A} + h.c.), \tag{S1}$$

where $c_{i,A}^{\dagger}$ ($c_{i,A}$) creates (annihilates) a fermion at site i and sublattice A. v and w correspond to the inter- and intra-cell hopping amplitudes, respectively. N corresponds to the number of unit cells. The model possesses topologically protected zero-energy modes when $v < w$.

The one-dimensional symmetry-reduced spectral localizer is given by [3]

$$L^{(1D)}_{\boldsymbol{\lambda}=(x,E)}(X, H) = [\kappa(X - xI) + i(H - EI)]\,\Gamma, \tag{S2}$$

where X is the position operator, κ is a scaling parameter with units of energy divided by length, and Γ is the chiral operator. Note that $L^{(1D)}_{\boldsymbol{\lambda}=(x,E)}(X, H)$ is only Hermitian at $E = 0$. As discussed in the main text, the localizer gap is given by $\mu_{\boldsymbol{\lambda}}(\boldsymbol{X}, H) = \min\{|\Sigma\,(L_{\boldsymbol{\lambda}}(\boldsymbol{X}, H))|\}$. Finally, the one-dimensional topological marker at a given position $\boldsymbol{\lambda} = (x, 0)$ corresponds to

$$\nu_x^L = \frac{1}{2}\mathrm{sig}[L^{(1D)}_{\boldsymbol{\lambda}=(x,0)}(X, H)], \tag{S3}$$

where $\mathrm{sig}[L^{(1D)}_{\boldsymbol{\lambda}=(x,0)}(X, H)]$ is the signature of the spectral localizer.

In zero dimensions, we can define the topological invariant directly from the Hamiltonian H (the same as the 1D case) [3], $\eta^L = \mathrm{sign}[\det(C)]$, where C is an real invertible matrix, and is obtained from H in the chiral basis as

$$H = \begin{pmatrix} 0 & C \\ C^T & 0 \end{pmatrix}. \tag{S4}$$

The corresponding 0D localizer gap corresponds to $\min\{|\Sigma\,(H)|\}$, the minimum absolute value of the Hamiltonian spectrum.

We now compute the localizer gaps and topological markers as a function of system size for $\kappa = 0.1(w/l)$, $w = 1$, $v = 0.5w$, and l is the site-to-site spacing, a parameter regime where the chain is topological. The 1D topological marker and associated 1D localizer gap as a function of position and the number of unit cells N are shown in Suppl. Fig. 1a,b. The chains have $2N$ sites. For chains with $N > 4$, there is a 1D localizer gap closing at the edges of the chain protecting the 1D topological phase with $|\nu^L_{\boldsymbol{\lambda}}| = 1$. The case $N = 4$ shows vanishing 1D localizer gaps, too small to yield robust 1D topology. For $N = 3$, the 1D localizer gap is closed, and for smaller systems, there is a nonzero gap, but the 1D topology is trivial, $|\nu^L_{\boldsymbol{\lambda}}| = 0$. Conversely, the 0D localizer gap increases as the number of unit cells decreases. In particular, at $N = 3$, the 0D gap protects the 0D topological marker $\eta^L = -1$. For a single unit cell, $N = 1$, the system is trivial. We note that the 0D localizer gap is too small for $N > 5$ to protect any meaningful 0D invariants.

The invariant in Eq. (S4) is basis-dependent, so one should not read much into the sign fluctuation in Suppl. Fig. 1c. Swapping the two elements in the even part of the graded basis will swap the sign of the determinant of C, for example. For a fixed Hilbert space this invariant can tell us when two class BDI Hamiltonians cannot be connected by a path that maintains the gap, but does not tell us which one is more trivial than the other.

Finally, we explore the effect of the parameter κ in this model. In particular, we consider the 0D localizer gap as a function of the number of unit cells N, along with the 1D localizer gap at the center of the chain, shown in Suppl. Fig. 2. We choose the center because it is the point where the gap is the most robust, thus providing an upper bound for the gap across the system. We find the same qualitative behavior, and similar quantitative behavior in the 1D localizer gap for choices of κ spanning three orders of magnitude.

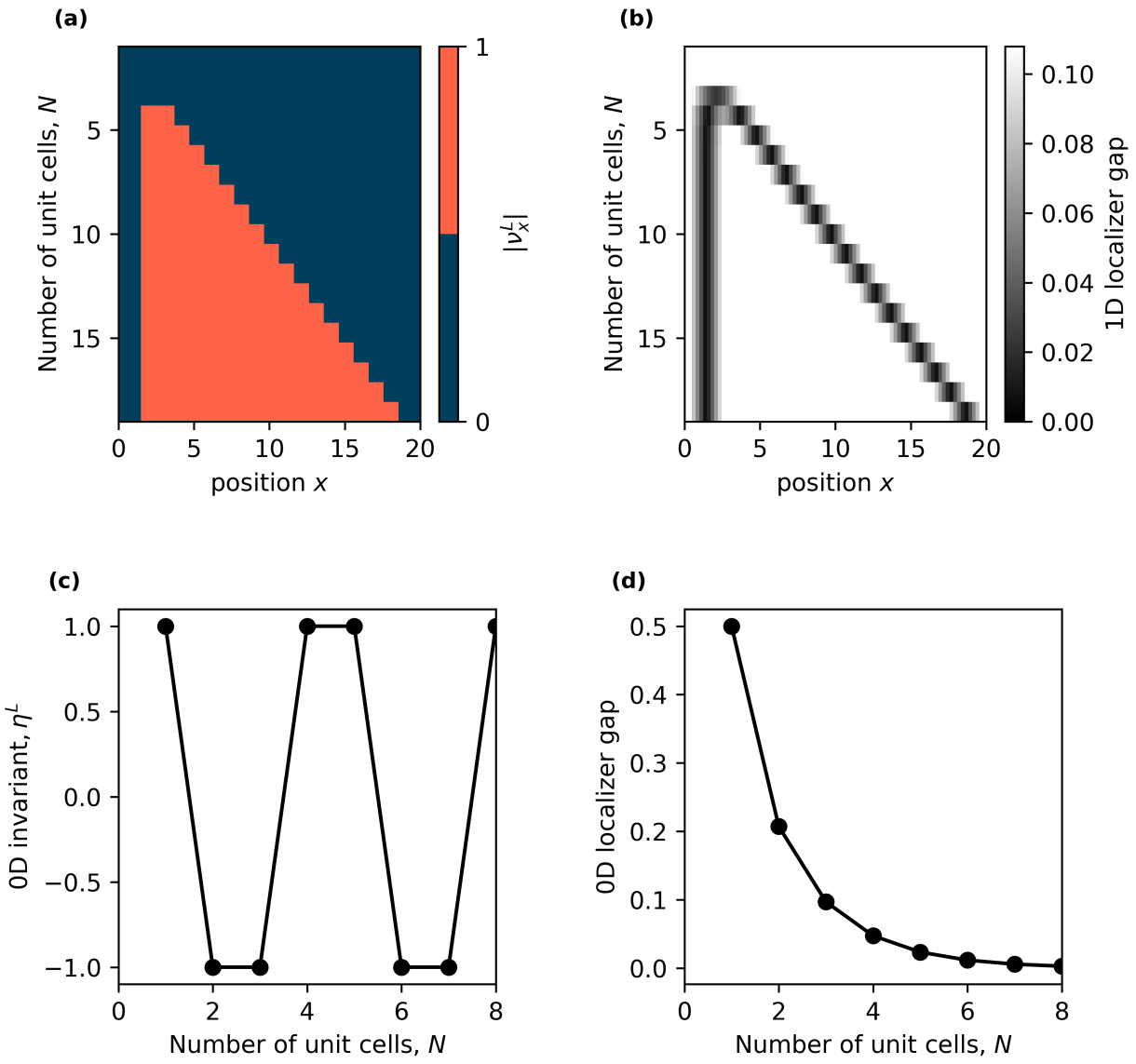

Supplementary Figure 1. (a) 1D topological marker $|\nu_x^L|$ and (b) 1D localizer gap as a function of position x and number of unit cells, N, for an SSH chain. The chains have $2N$ sites and we use the parameters $\kappa = 0.1w/l$, $w = 1$, and $v = 0.5w$. (c) 0D topological invariant, η^L, and (d) 0D localizer gap as a function of system size for the same parameters as panels (a-b).

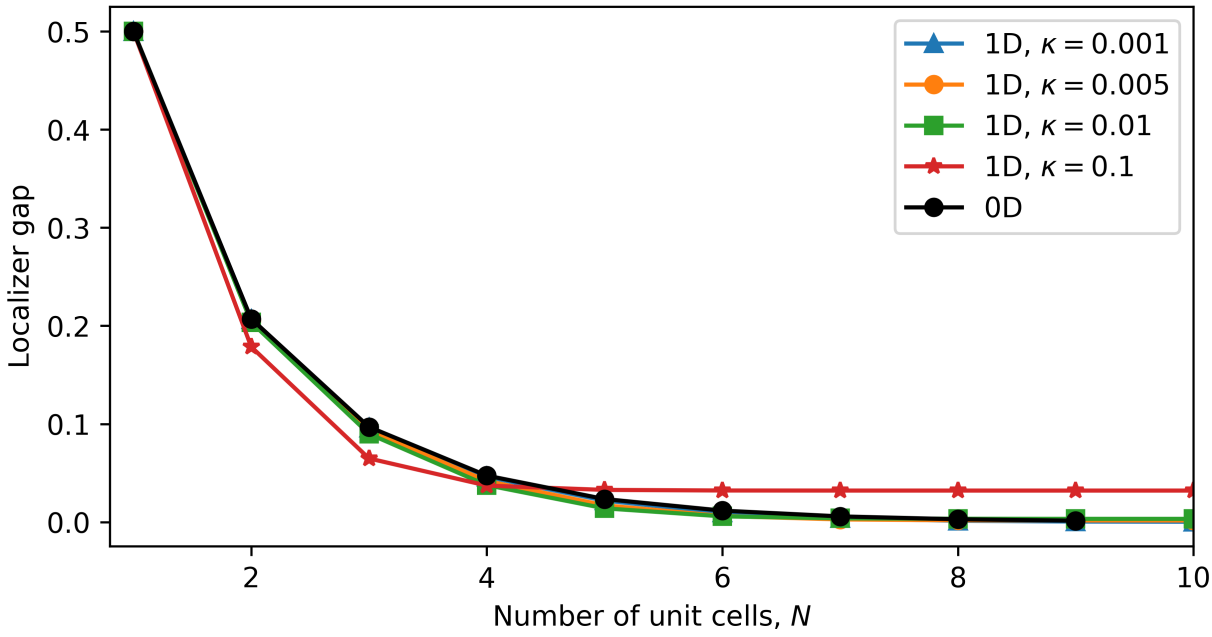

Supplementary Figure 2. Zero- and one-dimensional localizer gap as a function of the number of unit cells, N, for an SSH model. The 1D localizer gap was computed at the center of the system using four values for κ in units of w/l. The 0D case is independent of κ. We use the parameters $w = 1$ and $v = 0.5w$.

SUPPLEMENTARY NOTE 2. EXTENDED PHASE DIAGRAM FOR NEGATIVE CHEMICAL POTENTIAL

In this section, we expand the range of chemical potential μ values considered in Fig. 3 of the main text to also include negative values. Our analysis shows that the phase diagram is symmetric under $\mu \to -\mu$, see Suppl. Fig. 3.

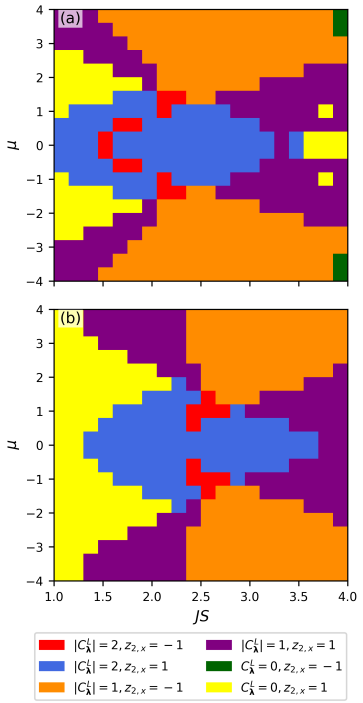

Supplementary Figure 3. Topological phase diagram at $E = 0$ as a function of the chemical potential μ and the product of the magnetic moment and exchange coupling JS, for $N = 20$, and spin-orbit coupling strength $\alpha = 0.45t/l$. The phase diagrams contain 20×20 points. (a) Phase diagram for $\Delta = 0.4t$. (b) Phase diagram for $\Delta = 1.2t$. As in the main text, the color code indicates the 2D local marker $|C^{\mathrm{L}}_{\boldsymbol{\lambda}}|$ computed at the center of a circular island, and the 1D local marker $z_{2,x}$ computed at the center of a chain using the same parameters and only changing the geometry. Topological transitions not captured in the diagram can occur as the geometry changes from 2D to 1D. The spectral localizer calculations use $\kappa = 0.05(t/l)$.

SUPPLEMENTARY NOTE 3. LOCAL MARKERS AS A FUNCTION OF THE PARAMETER κ

In this section, we show how our results depend on the parameter κ. In particular, we consider the phase diagram in Fig. 3 in the main text, and fix the chemical potential at $\mu = 1.5t$, as in involves topological transitions in both 1D and 2D as a function of JS. We then calculate the 1D topological marker $z_{2,x}$ and 1D localizer gap for a chain geometry, and the 2D topological marker $C^L_{\boldsymbol{\lambda}}$ and 2D localizer gap for an island geometry as a function of JS and κ. For both topological invariants, there is an order of magnitude of values for κ with a nonzero spectral localizer gap and well-defined topological marker, as shown in Suppl. Fig. 4, for $\Delta = 1.2t$. When we reduce the superconducting gap while keeping the system sizes the same, we expect the range of κ to decrease, as shown in Suppl. Fig. 5.

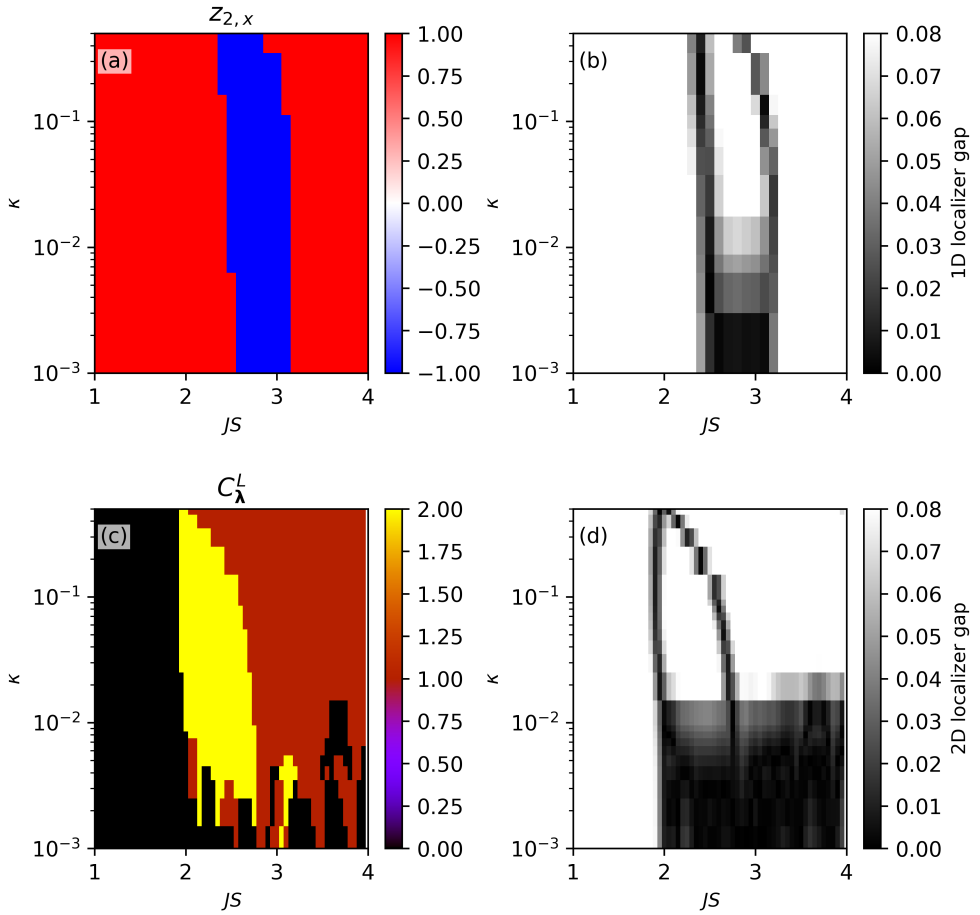

Supplementary Figure 4. (a) 1D topological marker $z_{2,x}$ and (b) 1D localizer gap for a chain geometry as a function of JS and κ computed at site $x = y = 10$ for a system with $N = 20$. (c) 2D topological marker $C^L_{\boldsymbol{\lambda}}$ and (d) 2D localizer gap for an island geometry as a function of JS and κ also computed at site $x = y = 10$. The rest of the parameters are $\mu = 1.5t$, $\alpha = 0.45t/l$, and $\Delta = 1.2t$.

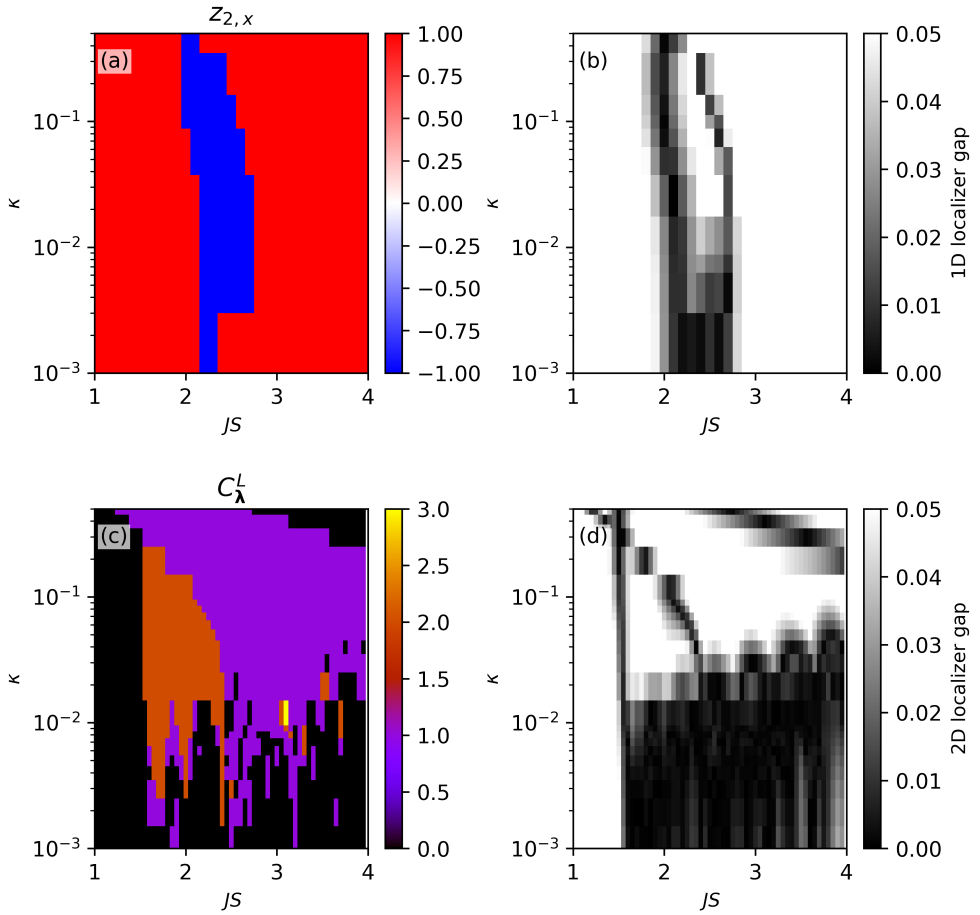

Supplementary Figure 5. (a) 1D topological marker $z_{2,x}$ and (b) 1D localizer gap for a chain geometry as a function of JS and κ computed at site $x = y = 10$ for a system with $N = 20$. (c) 2D topological marker $C^L_{\boldsymbol{\lambda}}$ and (d) 2D localizer gap for an island geometry as a function of JS and κ also computed at site $x = y = 10$. The rest of the parameters are $\mu = 1.5t$, $\alpha = 0.45t/l$, and $\Delta = 0.4t$.

SUPPLEMENTARY NOTE 4. LOCAL DENSITY OF STATES

In this section, we present the local density of states as a function of position at $E = 0$ for all the geometries depicted in Fig. 4 of the main text, see Suppl. Fig. 6.

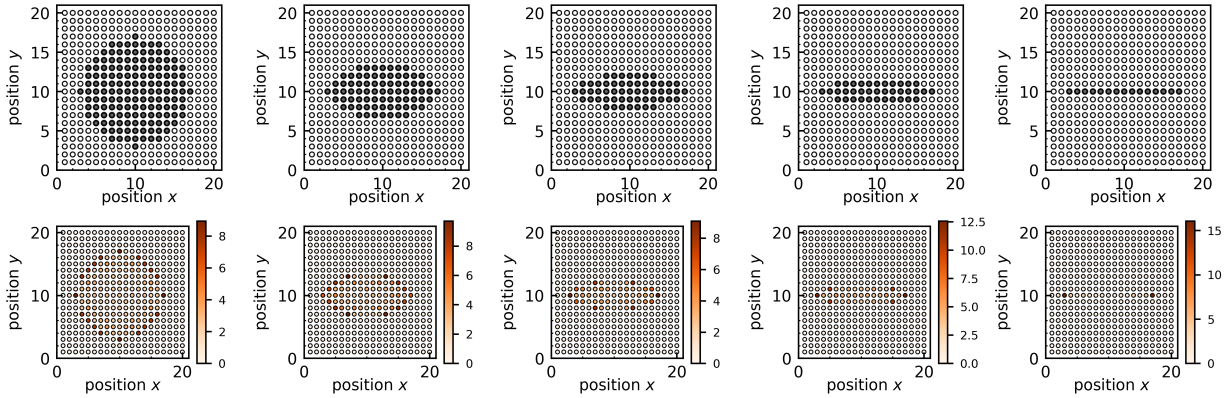

Supplementary Figure 6. Local density of states for the full set of Shiba geometries considered in Fig. 4 of the main text, with $\alpha = 0.45t/l$, $\Delta = 2.0t$, $SJ = 4.8t$, $\kappa = 0.05(t/l)$ and $N = 20$.

SUPPLEMENTARY NOTE 5. SHIBA ISLAND WITH $|C^{\mathrm{L}}_{\boldsymbol{\lambda}}| = 2$ TRANSITIONING INTO A TRIVIAL CHAIN, WITH $z_{2,x} = 1$

In this section, we consider the case of a Shiba island with $|C^{\mathrm{L}}_{\boldsymbol{\lambda}}| = 2$ transitioning into a trivial chain, with $z_{2,x} = 1$, see Suppl. Fig. 7. The topological dimensional crossover occurs for the three-atoms-wide island, analogous to the cases discussed in the main text, but in this case the 1D system is trivial.

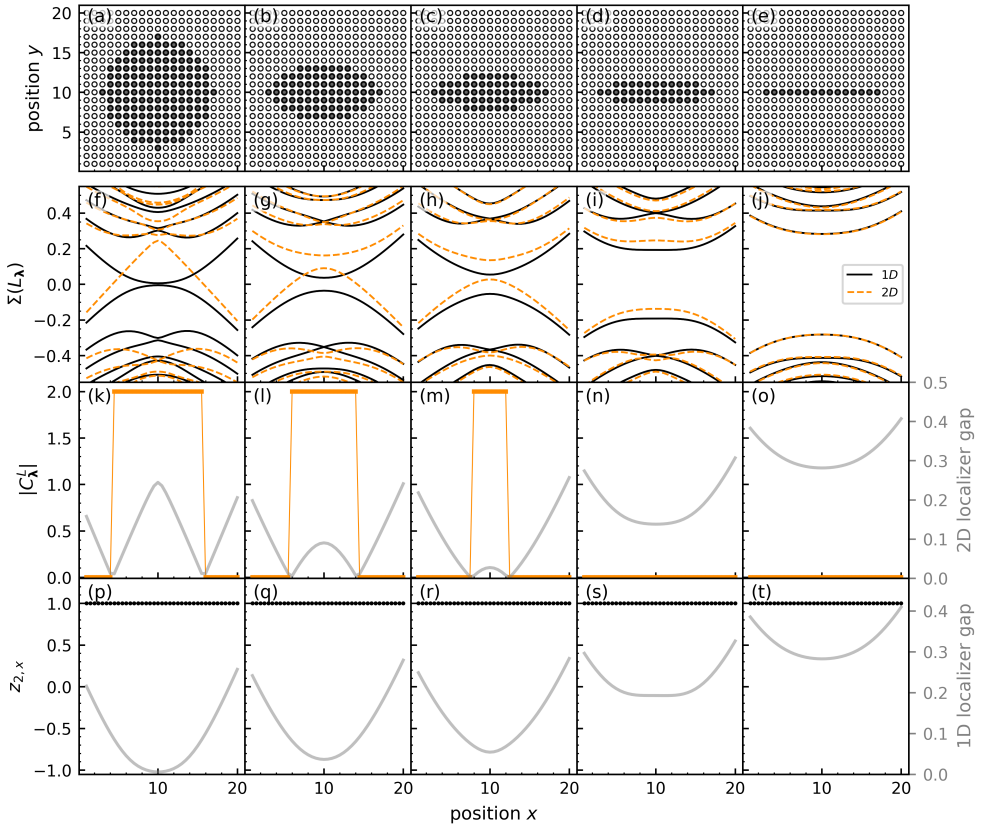

Supplementary Figure 7. (a)-(e) Arrangement of magnetic adatoms interpolating from the two-dimensional circular island to the one-dimensional chain. (f)-(j) 1D (black solid line) and 2D (dashed orange lines) localizer spectrum $\Sigma(L_{\boldsymbol{\lambda}})$ as a function of position x for $y = N/2$. (k)-(o) Local Chern number, $|C^{\mathrm{L}}_{\boldsymbol{\lambda}}|$, (orange squares) and 2D localizer gap $\min\{|\Sigma(L^{(2D)}_{\boldsymbol{\lambda}})|\}$ (solid gray line) as a function of position x for $y = N/2$. (p)-(t) Local $z_{2,x}$ invariant (black circles) and 1D localizer gap $\min\{|\Sigma(L^{(1D)}_{\boldsymbol{\lambda}})|\}$ (solid gray line) as a function of position x for $y = N/2$. The parameters used are $N = 20$, $\mu = 0$, $\alpha = 0.8t/l$, $\Delta = 1.2t$, and $JS = 2t$. The spectral localizer calculations use $\kappa = 0.05(t/l)$.

SUPPLEMENTARY NOTE 6. SHIBA ISLAND WITH $|C^{\mathrm{L}}_{\boldsymbol{\lambda}}| = 0$ TRANSITIONING INTO A TOPOLOGICAL CHAIN, WITH $z_{2,x} = -1$

In this section, we consider the case of a Shiba island with $|C^{\mathrm{L}}_{\boldsymbol{\lambda}}| = 0$ that transitions into a topological chain upon dimensional crossover, with $z_{2,x} = -1$, see Suppl. Fig. 8. This case corresponds to one of the dark green areas in the topological phase diagram [Fig. 3d of the main text]. The topological dimensional crossover occurs for the three-atoms-wide island.

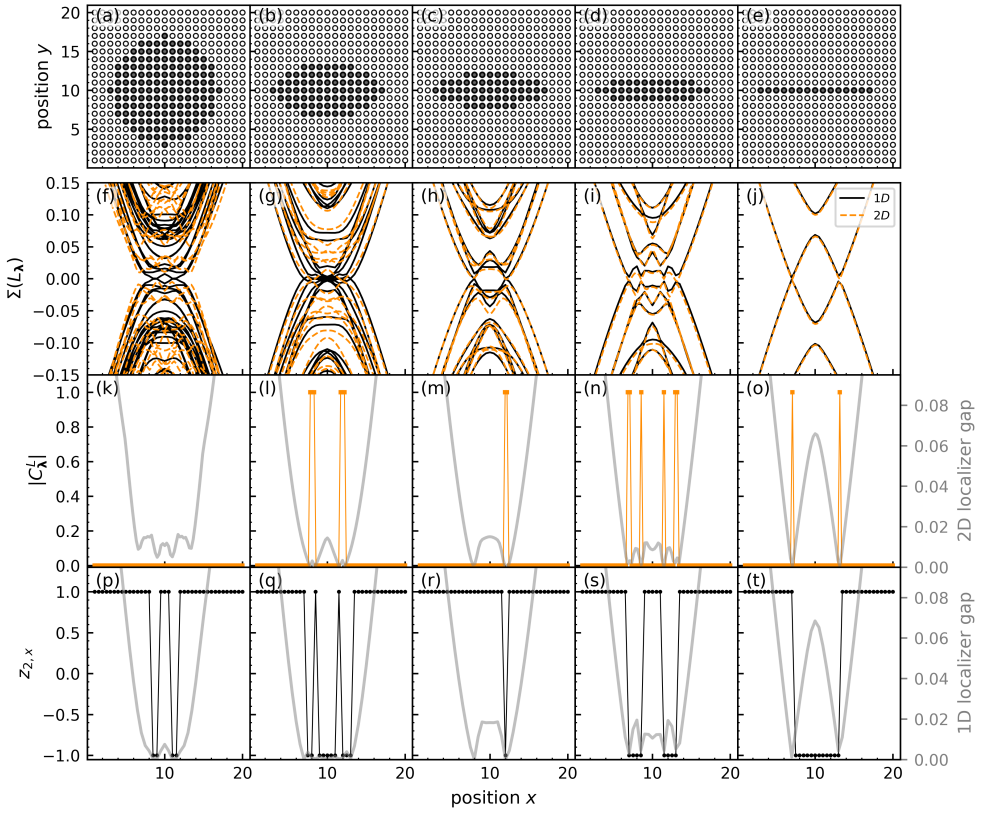

Supplementary Figure 8. (a)-(e) Arrangements of magnetic adatoms interpolating from the two-dimensional circular island to the one-dimensional chain geometries. (f)-(j) 1D (black solid line) and 2D (dashed orange lines) localizer spectrum $\Sigma(L_{\boldsymbol{\lambda}})$ as a function of position x for $y = N/2$. (k)-(o) Local Chern number, $|C^{\mathrm{L}}_{\boldsymbol{\lambda}}|$, (orange squares) and 2D localizer gap $\min\{|\Sigma(L^{(2D)}_{\boldsymbol{\lambda}})|\}$ (solid gray line) as a function of position x for $y = N/2$. (p)-(t) Local $z_{2,x}$ invariant (black circles) and 1D localizer gap $\min\{|\Sigma(L^{(1D)}_{\boldsymbol{\lambda}})|\}$ (solid gray line) as a function of position x for $y = N/2$. The parameters are $N = 20$, $\mu = 4.0t$, $\alpha = 0.45t/l$, $\Delta = 0.4t$, and $JS = 4t$. The spectral localizer calculations use $\kappa = 0.05(t/l)$.

SUPPLEMENTARY REFERENCES

[1] N. Lera and J. V. Alvarez, Mechanical topological insulator in zero dimensions, Phys. Rev. B **97**, 134118 (2018).

[2] W. P. Su, J. R. Schrieffer, and A. J. Heeger, Solitons in polyacetylene, Phys. Rev. Lett. **42**, 1698 (1979).

[3] T. A. Loring, K-theory and pseudospectra for topological insulators, Annals of Physics **356**, 383 (2015).